Journal of Biomedical Optics

SPIEDigitalLibrary.org/jbo

Dependence of optical scattering from Intralipid in gelatin-gel based tissue-mimicking phantoms on mixing temperature and time

Puxiang Lai
Xiao Xu
Lihong V. Wang

Dependence of optical scattering from Intralipid in gelatin-gel based tissue-mimicking phantoms on mixing temperature and time

Puxiang Lai,[†] Xiao Xu,[†] and Lihong V. Wang[*]
Washington University in St. Louis, Department of Biomedical Engineering, Optical Imaging Laboratory, St. Louis, Missouri 63130-4899

Abstract. Intralipid is widely used as an optical scattering agent in tissue-mimicking phantoms. Accurate control when using Intralipid is critical to match the optical diffusivity of phantoms to the prescribed value. Currently, most protocols of Intralipid-based hydrogel phantom fabrication focus on factors such as Intralipid brand and concentration. In this note, for the first time to our knowledge, we explore the dependence of the optical reduced scattering coefficient (at 532 nm optical wavelength) on the temperature and the time of mixing Intralipid with gelatin-water solution. The studied samples contained 1% Intralipid and were measured with oblique-incidence reflectometry. It was found that the reduced scattering coefficient increased when the Intralipid-gelatin-water mixture began to solidify at room temperature. For phantoms that had already solidified completely, the diffusivity was shown to be significantly influenced by the temperature and the duration of the mixing course. The dependence of the measured diffusivity on the mixing conditions was confirmed by experimental observations. Moreover, the mechanism behind the dependence behavior is discussed. [DOI: 10.1117/1.JBO.19.3.035002]

Keywords: tissue-mimicking phantom; lipid emulsions; gelatin gel; optical reduced scattering coefficient; optical absorption coefficient; oblique-incidence reflectometry; dynamic light scattering.

Paper 130845R received Dec. 3, 2013; revised manuscript received Feb. 11, 2014; accepted for publication Feb. 12, 2014; published online Mar. 6, 2014.

1 Introduction

Tissue-mimicking phantoms are widely used in biomedical optics research for system validation, optimization, calibration, stability evaluation, and quantitative studies.[1] They can be easily fabricated with controlled geometries, homogeneities, and physical properties. Depending on specific applications, phantoms use various types of materials as the bulk matrix, such as aqueous suspensions,[2,3] gelatin/agar/polyacrylamide-based hydrogels,[4,5] polyester/epoxy/polyurethane-based resins,[6–8] and room temperature vulcanizing silicone.[9] Absorbing (e.g., India ink, whole blood, and Evans blue) and scattering (e.g., Intralipid, polystyrene microspheres, and white metal oxide powders) agents can then be mixed into the phantom matrix to emulate the optical properties (such as the absorption coefficient μ_a and the reduced scattering coefficient μ_s') of real tissues.[1]

Intralipid is a scattering agent broadly used in phantoms to reproduce the optical scattering coefficient μ_s and the anisotropy coefficient g of real tissues. Intralipid is biologically similar to the bilipid membrane of cells and organelles[1,10]—the major constituents causing optical scattering in tissue. Its main scatterers, lipids, have a particle size on the order of 100 nm.[1,3,11,12] When Intralipid is added to the bulk matrix, the resulting scattering coefficient μ_s and the reduced scattering coefficient μ_s' $[\mu_s' = \mu_s(1-g)]$ of the phantom have a linear dependency on the Intralipid concentration.[13,14] For example, at 751-nm wavelength, μ_s' is measured to be around 100, 200, and 300 cm^{-1} for 10%, 20%, and 30% Intralipid solutions, respectively.[14] In addition, Intralipid has negligible absorption in the visible spectral region,[14,15] and a refractive index close to that of soft tissue.[1,16] Further, the optical properties of Intralipid from different production batches or vendors have little variation.[4,14,15,17] These features, together with its low cost and wide availability, have made Intralipid the chosen diffusive reference standard for many phantom studies.[14,15] As a common practice, Intralipid-based phantoms can be made to simulate the optical properties of different types of tissues by varying the concentrations of the scatterer—Intralipid and the absorber, such as India ink.[1,11]

Intralipid phantoms exist as either aqueous solutions or hydrogels. Many of the studies characterizing Intralipid's optical properties were performed on its aqueous solution, in which case Intralipid can be easily mixed well with the matrix to form a stable emulsion having the designed scattering and absorption properties. In circumstances where a static matrix with limited water mobility or with complex sample structures is desired, hydrogels, such as gelatin gel, are preferred.[18–23] Fabrication of such hydrogel phantoms with Intralipid additive is nontrivial—the main variables being the mixing temperature and time. To mix Intralipid thoroughly with hydrogel in the liquid phase, e.g., a gelatin-water solution, the mixture has to be kept warm to prevent the hydrogel matrix from solidifying.[20,24] For a complex phantom with multiple parts,[6,19] its fabrication usually takes several steps, during which the Intralipid and the matrix must remain liquid. Therefore, an Intralipid-gelatin-water mixture could stay on a hot/stirring plate for up to 1 to 2 h when a phantom is being made.

In previous studies, the optical properties of Intralipid hydrogel phantoms were assumed to be no different from those of

*Address all correspondence to: Lihong V. Wang, lhwang@wustl.edu

†Equal contribution.

aqueous solution phantoms. This presumption, however, contradicts our experimental observation: when the mixing temperature is high and/or the mixing time is long, lipid droplets start to amalgamate near the Intralipid-gelatin-water mixture surface, indicating a separation of the optical scatters (lipids) from the matrix. This separation is irreversible, even when the temperature is lowered. As a result, the top surface of the solidified gel phantom may appear more opaque than the body beneath. In contrast, in an Intralipid-water solution, some lipid droplets will separate from water if the mixture temperature becomes too high, but when the temperature drops, they will disperse evenly to form a homogeneous emulsion again.[1,25] In this paper, for the first time to our knowledge, we explore how the temperature and time of mixing Intralipid with gelatin-water solution influence the resulting hydrogel's optical scattering property.

2 Materials and Methods

2.1 *Reagents*

Gelatin from porcine skin (#G2500-1kG; gel strength 300, Type A) was purchased from Sigma–Aldrich, St. Louis, Missouri. Intralipid® 20% was manufactured by Fresenius Kabi, Uppsala, Sweden, and was purchased from VWR International, Batavia, Illinois (#68100-276). Sodium azide (#S2002-100G) was purchased from Sigma–Aldrich, St. Louis, Missouri. Ultrapure, deionized, and degassed water were used for all solutions.

2.2 *Phantom Preparation*

Two types of Intralipid phantoms (Table 1) were studied. The first type (Groups 1 to 4) was Intralipid hydrogel phantoms made from Intralipid (1% by weight), gelatin (10%), and water (89%). The second type (Groups 5 to 7) was Intralipid aqueous solution phantoms made from Intralipid (1%) and water (99%). The concentration of 1% of Intralipid was chosen to obtain a μ_s' of $\sim 10\ \mathrm{cm}^{-1}$ (i.e., a transport mean free path $l_{\mathrm{tr}} \approx 1/\mu_s'$ of ~ 1 mm),[3,26] which reasonably mimics that of the whole milk ($l_{\mathrm{tr}} = 1.0 \pm 0.1$ mm) and the pork breast ($l_{\mathrm{tr}} = 1.2 \pm 0.2$ mm).[11]

To fabricate the Type I samples, we adapted the protocol from Ref. 27 with improved temperature and time control:

1. Add porcine gelatin to ultrapure, deionized, and degassed water at the specified concentration. Place the mixture in a glass beaker on a hot/stirring plate (Barnstead Thermolyne, Model SP18425).
2. Heat the mixture of gelatin and water to a temperature (37 to 50°C, corresponding to a heater setting of 3 to 5) above the gelatin's melting point of ~35°C. Throughout heating, stir with a magnetic stirring bar at a constant speed (a stirrer setting of 4 to 5) until the gelatin dissolves completely and the solution turns transparent [Fig. 1(a)].
3. Add sodium azide to the solution at a concentration of 15 mM to preserve the hydrogel.[20,28]
4. Add an appropriate amount of Intralipid into the gelatin-water solution, water-bathed in a larger beaker [Fig. 1(b)], and stir at the conditions specified in Table 1. Monitor the water bath temperature with a thermometer. To minimize vapor loss during the mixing process, keep the beakers covered with an aluminum foil.[24]
5. Fill cylindrical molds with the final solution, and let the hydrogel solidify at room temperature (20°C).

Table 1 Preparation conditions for samples used in this study.

Type	Group	No. of samples examined	Mixing temperature (°C)	Mixing time (min)
I Intralipid+ gelatin + water	1	1	38	30
	2	6	34 to 95	30
	3	9	40	10 to 150
	4	9	37	10 to 150
II Intralipid+ water	5	6	34 to 95	30
	6	9	40	10 to 150
	7	9	37	10 to 150

The procedure to make the Type II samples was similar, except that no gelatin or sodium azide were added, and the mixtures did not gel.

After fabrication, the reduced optical scattering coefficient μ_s' of the Type I samples was measured using oblique-incidence reflectometry (OIR).[29] For the Group 1 sample, the measurement was taken during the gelling process at room temperature (20°C). Other samples, after they solidified at room temperature, were stored in sealed zip bags in a refrigerator (temperature set at 4°C) for at least 12 h before measurements. These storage conditions ensured complete crosslinking (gelling).[24]

2.3 *Optical Scattering Measurement Using Oblique-Incidence Reflectometry*

The cylindrical molds containing the Intralipid hydrogel samples were sufficiently large (6 cm in diameter and 6 cm in depth) to justify the approximation of treating the phantoms as semi-infinite turbid media. Furthermore, the optical absorption coefficient μ_a of the phantoms was much smaller than the reduced scattering coefficients μ_s'. Therefore, OIR[29] could be used to the measure μ_s' of the samples accurately.

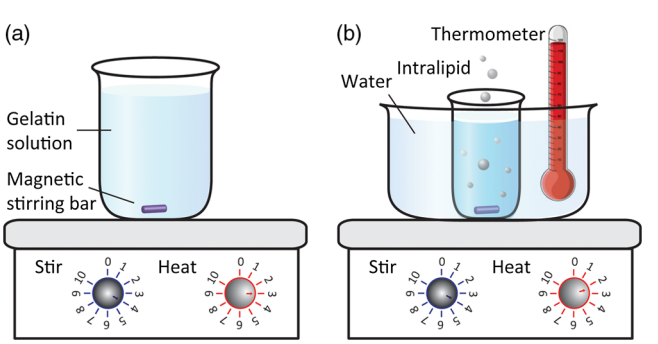

Fig. 1 (a) Illustration of the preparation of gelatin-water solution. (b) Illustration of mixing Intralipid with the prepared gelatin-water solution, with controlled temperature and duration.

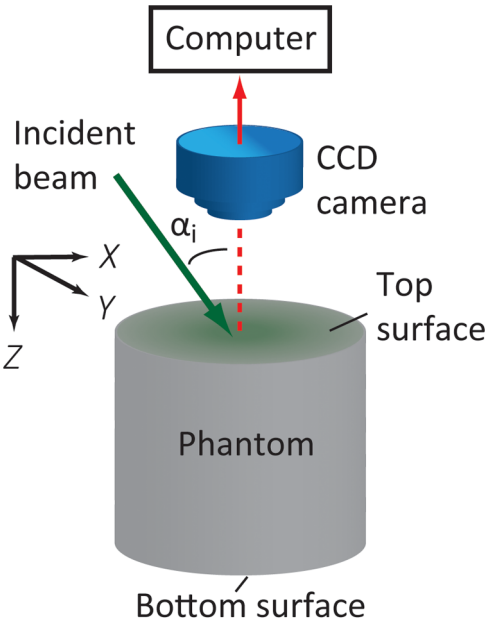

Fig. 2 Schematic of the oblique-incidence reflectometer used to measure the reduced scattering coefficient of the prepared phantoms. *XYZ* are system coordinates.

Figure 2 shows a schematic of the OIR experimental setup. An attenuated 1-mm diameter beam from a 532 nm laser source (Coherent, Verdi V-5, Santa Clare, California) illuminated the phantom surface at an angle α_i. A CCD camera (Andor Technology, iStar 734, Belfast, United Kingdom) was mounted above the phantom to image the diffuse reflectance of the incident beam. An example of the two-dimensional diffuse reflectance pattern captured by the CCD is given in Fig. 3(a). In Fig. 3(b), the light intensity distribution along the dashed line in Fig. 3(a) is represented as curve M. Curve C is the center of the symmetrical reflectance profile and Δx is the horizontal distance between C and the point of incidence. According to Refs. 29 and 30,

$$\Delta x = \frac{\sin \alpha_i}{n_{\text{sample}}(0.35\mu_a + \mu_s')}, \tag{1}$$

where n_{sample}, the refractive index of the Intralipid hydrogel, was approximated to be 1.33, which could be measured with a clear gelatin gel containing no Intralipid. This approximation is justified since both gelatin and Intralipid have refractive indexes close to that of water ($n_{\text{water}} = 1.33$).[4,16] The angle α_i was measured to be 37.9 deg, and μ_a of a clear gelatin gel was measured to be 0.12 cm^{-1} by a spectrophotometer (Varian, Cary 50, Palo Alto, California). Note that the absorption due to 1% Intralipid is negligible.[31] Therefore, once Δx was determined from the sample's reflectance pattern, as shown in Fig. 3, the reduced scattering coefficient can be calculated by

$$\mu_s' = \frac{\sin \alpha_i}{n_{\text{water}}\Delta x} - 0.35\,\mu_a. \tag{2}$$

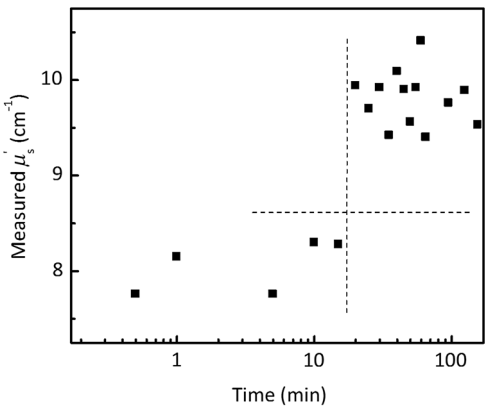

Fig. 4 Measured reduced scattering coefficient as a function of time for the Group 1 sample during the cooling process at room temperature (20°C). The dashed lines are to highlight two different phases before and after solidifications.

3 Results

For the Group 1 sample, right after the Intralipid-gelatin-water mixture was poured into the cylindrical mold, we started to record the OIR pattern until the phantom solidified completely. The values of μ_s' calculated from the reflectance patterns are shown in Fig. 4 as a function of time during the gelling process at room temperature. As can be seen, μ_s' was around 8.0 cm^{-1} or slightly higher in the beginning, and increased to 9.5 to 11 cm^{-1} when the hydrogel began to solidify after ~20 min.

In Groups 2 to 4, samples were completely solidified and taken out of their molds before the OIR measurements, enabling

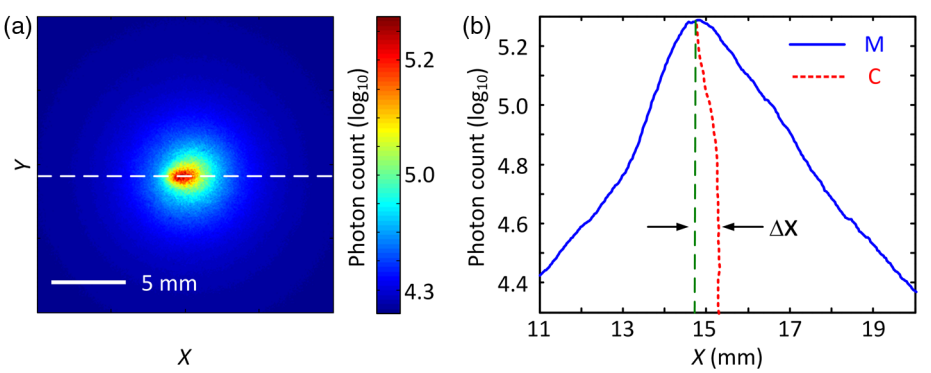

Fig. 3 (a) An example of the oblique incidence diffuse reflectance pattern. The length of the scale bar is 5 mm. (b) Curve M is the light intensity (photon count) distribution profile along the dashed line in (a), and curve C is composed of the midpoints of the left and right sides of M for specific photon counts. Δx is the horizontally shifted distance between the vertical portion of curve C and the point of incidence.

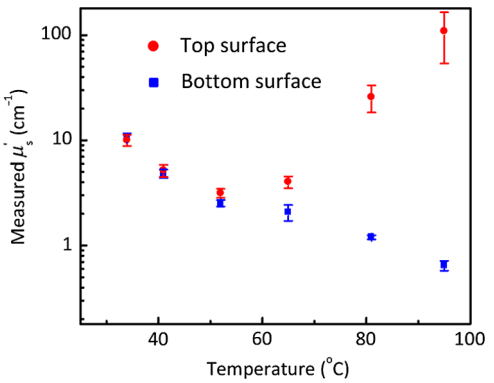

Fig. 5 Measured reduced scattering coefficients for Group 2 samples, which were prepared with different mixing temperatures but the same duration (30 min). For each phantom, both the top (red circles) and bottom (blue squares) surfaces were examined. On each surface, five measurements were performed at five different locations, from which a mean value was obtained as the mean μ_s' for that surface. The standard deviation is represented by the error bars.

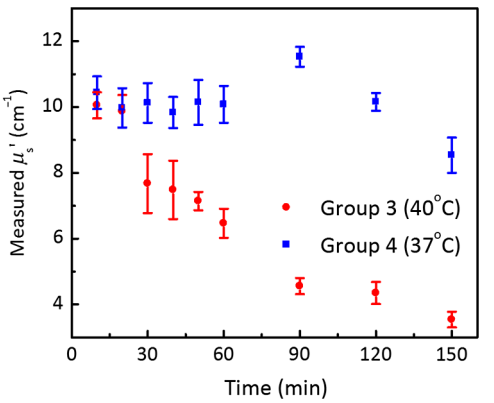

Fig. 6 Measured reduced scattering coefficients for Groups 2 and 3 samples, prepared with different mixing durations but the same temperatures, at 40°C (red circles) and 37°C (blue squares), respectively. Note that results from only the bottom surfaces are shown here.

us to examine both the top and the bottom surfaces of the phantoms. To reduce the measurement error caused by sample inhomogeneity, we recorded the reflectance patterns from five different spots on each surface.

In Fig. 5, the calculated μ_s' based on the reflectance patterns of the Group 2 samples is shown as a function of mixing temperature. As we can see $\mu_s' \approx 10$ cm^{-1} when the mixing temperature was 34°C, and dropped to ~5.0 cm^{-1} when the temperature was 41°C. At these temperatures, the OIR measurements performed at different spots of both top and bottom surfaces yielded consistent μ_s' values, indicating optical homogeneity of the phantoms. This homogeneity, however, started to break down at higher mixing temperatures. μ_s' measured from the bottom surface decreased monotonically from 2.5 cm^{-1} at 52°C to 0.65 cm^{-1} at 95°C, while μ_s' measured from the top surface increased monotonically from 3.2 cm^{-1} at 52°C to >100 cm^{-1} at 95°C. Moreover, measurements from the top at higher temperatures had much larger error bars, suggesting increased optical inhomogeneity.

In Groups 3 and 4, samples were prepared with the same mixing temperatures (40°C from Group 3 and 37°C from Group 4), but different mixing times. μ_s' was measured at the samples' bottom surfaces, and is shown in Fig. 6 as a function of mixing time. At the 40°C mixing temperature, $\mu_s' \approx 10$ cm^{-1} when the mixing time was <20 min. As the mixing time increased, μ_s' became inversely related to the duration. However, at a mixing temperature lower than 40°C, μ_s' remained relatively constant around 10 cm^{-1} over a long period, until the mixing time exceeded 150 min, in which case μ_s' decreased to 8.5 cm^{-1}.

4 Discussion

The objective of this study was to explore the influence of the mixing temperature and duration on the resulting optical diffusivity when the Intralipid was used as the scatterer in gelatin-based tissue-mimicking hydrogel phantoms.

In Fig. 4, we showed μ_s' as a function of time for the Group 1 sample. The investigated period covered the cooling process from the initial 38°C to the final 20°C, and the formation/reinforcement of crosslinking (solidification) after ~20 min. The dependence of μ_s' on the measured time, and consequentially the measured temperature, is potentially related to two factors. First, the reduction in mixture volume—measured to be <2%—following the solidification increases the scatterer concentration and results in a higher μ_s'.[32] Second, the refractive index of water changes with the measured temperature,[33] which alters the mismatch of refractive index between the Intralipid particles and the water, and introduces variations in μ_s'.[31]

In Fig. 5, we presented the measured μ_s' from the solidified Group 2 samples at room temperature. Apparently, the samples' diffusivity was affected by the temperature when mixing Intralipid with the hydrogel. Moreover, samples made with relatively high mixing temperatures showed increased divergence between measurements implemented at the top and bottom surfaces. As seen, the measured μ_s' at the bottom surface decreased as a function of mixing temperature, but those measured at the top decreased first, then later increased dramatically with high mixing temperatures. Such variations of μ_s' primarily arise from the change of particle concentration of the lipid droplets, the main constituents that contribute scattering in fat emulsions. Usually, these fat emulsions are quite stable when mixed with water, but the addition of gelatin (a type of collagen) destabilizes the emulsions.[34] As a result, some of the lipid droplets, initially evenly distributed throughout the scattering mixture, may flocculate, aggregate, and coalesce.[35] Eventually, some lipid droplets can be deemulsified, forming two separate layers: the dispersed droplets float on the top, leading to enlarged but inhomogeneous μ_s'; the continuous (homogenous) phase that has a reduced concentration of lipid droplets remains in the lower portion remains, and has a correspondingly lower μ_s'.

The above hypothesis can be further verified if we look at the photos of two samples from Group 2 (Fig. 7), processed with mixing temperatures of 34 and 95°C, respectively. The first sample (mixed at 34°C) is relatively uniform [Fig. 7(a)], but the second (mixed at 95°C) has a top surface different from the other fractions of the volume [Fig. 7(b)]. The lower portion of the second sample is more transparent than that of the first one, suggesting a lower concentration of lipid droplets. On the other hand, the top surface of the second sample appears to be whiter but more uneven [Fig. 7(d)] than that of the first sample [Fig. 7(c)], indicating increased diffusivity and inhomogeneity. All these observations are consistent with the measurements in Fig. 5 and the hypothesis.

It is further shown, in Fig. 6, that the occurrence and degree of phase separation are also affected by the duration of the

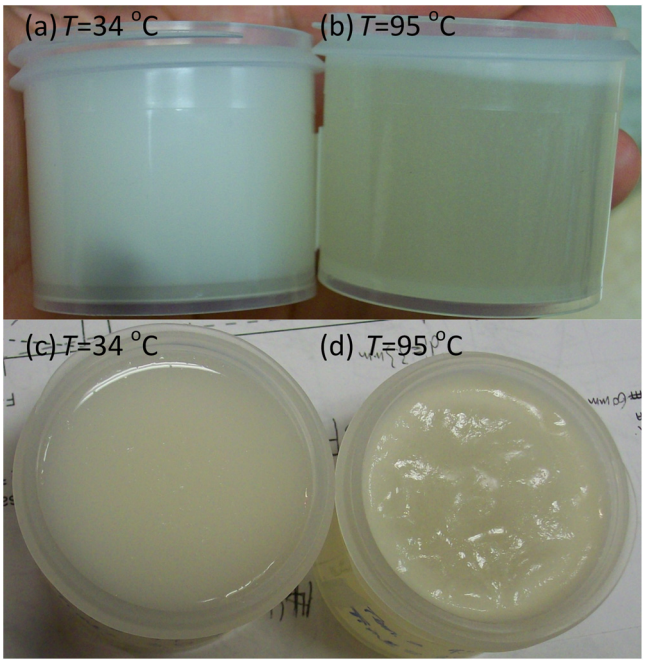

Fig. 7 Photographs of two solidified phantoms from Group 2, with the same mixing time length of 30 min but different mixing temperatures (34°C and 95°C, respectively), before they were removed from the sample molds. (a) and (b) are viewed from the side, while (c) and (d) are from the top.

mixing process, even when the mixing temperature is moderate (e.g., 40°C). However, if the mixing temperature is further reduced, say, down to human body temperature (37°C) or even lower, the effect of phase separation can be minimized and a relatively constant μ_s' can be maintained within a mixing course of 2 h. This finding is particularly important when preparing a time-consuming complex sample requiring uniform diffusivity among different compartments.

However, μ_s' variations shown in Figs. 5 and 6 might also be associated with changes of lipid droplet size—if the changes indeed happened. To confirm this possibility, we also measured the diffusivity and the droplet diameter of Type II samples (Groups 5 to 7) that were prepared under the conditions specified in Table 1. In our study, the measurement of particle diameter was performed with dynamic light scattering (DLS) equipment (Malvern Instruments, Zetasizer Nano ZS, Worcestershire, UK), which handles only aqueous solution. Therefore, no gelatin was added to samples in Groups 5 to 7. Right before measurements of both diffusivity and particle size, these samples were remixed to ensure sample homogeneity. The measured μ_s' from all these samples was between 9.0 and 11 cm^{-1}, confirming the previous reports[25,31] on the diffusivity of Intralipid-water samples. Figure 8(a) is an example of a lipid droplet size distribution histogram measured by the DLS method. In Fig. 8(b), the measured diameters from all Type II samples are shown and sorted according to their groups. Clearly, the diameters of lipid droplets are fairly constant (most are between 200 and 400 nm) from sample to sample, regardless of the differences in mixing conditions. This behavior is in good agreement with the literature,[1,3,11,12,25] confirming that in Intralipid-water solution, even deemulsification occurs, when temperature drops, lipid droplets could disperse evenly again to form a homogenous aqueous solution. This reversibility, however, is not seen in gelatin hydrogels (Figs. 5–7). Since the DLS equipment can only characterize aqueous solutions, we were not able to directly measure the Intralipid particle sizes at different mixing conditions for gelatin gel-based samples. Nevertheless, the μ_s' changes in samples in Groups 2 to 4 were mainly related to the particle concentration variation caused by phase separation, as discussed earlier.

It needs to be pointed out that two minor factors in the current study potentially cause inaccuracies in the measurements of μ_s'. First, in our calculation [Eqs. (1) and (2)], the refractive index of water at 20°C and 1 bar was used to represent the refractive index of the whole sample. Because the refractive indexes of gelatin and Intralipid do not differ much from that of water, this is a fair approximation when water is the dominant constituent. The other potential inaccuracy emerges when the μ_s' of the measured sample is very high: x (the horizontal shift between the center of symmetrical reflectance profile and the point of incidence) then might be too small to be determined precisely. However, the overall measurement accuracy based on the OIR method is reasonably accurate.[29] More importantly, in the current study, we are more interested in the relative changes, rather than the absolute magnitudes, of the resulting μ_s'. Thus, the two sources of inaccuracy mentioned above do not severely degrade the rigor of the investigation or the derived conclusions.

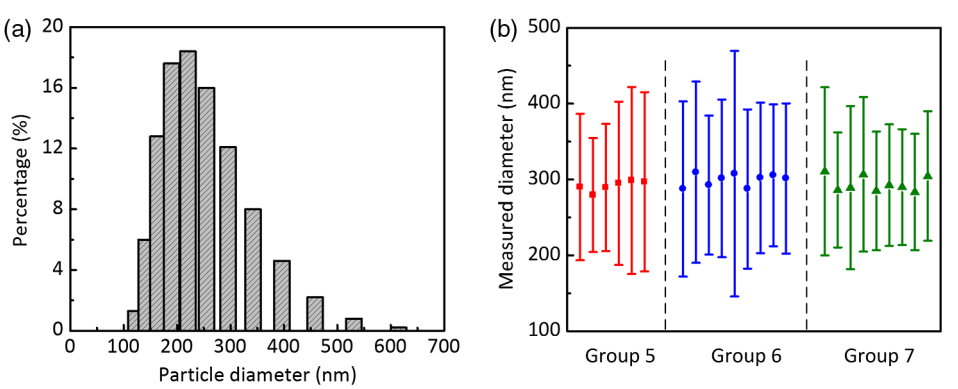

Fig. 8 (a) An example of lipid droplet size distribution measured by the dynamic light scattering method. (b) Measured lipid droplet size of samples in Groups 5 to 7. Each point is the mean diameter of particle size of a measured sample (red squares for Group 5 samples, blue circles for Group 6 samples, and green triangles for Group 7 samples). The error bar is the standard deviation of the size distribution shown in (a).

5 Conclusion

Our work was spurred by the experimentally observed irreversible inhomogenization of optical diffusivity in the fabrication of Intralipid-gelatin-water phantoms. We investigated the effect of mixing temperature and duration on the phantom's reduced optical scattering coefficient μ_s' quantitatively, using OIR. It was found that high temperature and prolonged mixing time increasingly caused phase separation in the Intralipid-gelatin-water emulsion, resulting in a decreasing μ_s'. On the other hand, the optical diffusivity of the Intralipid-water emulsion remains constant regardless of the mixing temperature or mixing time, as confirmed by the measurement of μ_s' and the optical scatterer sizes using OIR and DLS. We, therefore, suspect that the phase separation in the Intralipid-gelatin-water emulsion was caused by irreversible changes of the Intralipid–gelatin structure at a higher temperature or a longer mixing time. Further investigation can clarify this matter, but is outside the scope of this paper. To fabricate Intralipid-gelatin-water phantoms having optical diffusivity that is consistent with that of Intralipid-water counterparts,[25,31] we found it is crucial to maintain the mixing temperature below 37°C and use mixing times not exceeding 2 h. We recommend our modified protocol for making Intralipid-gelatin-water phantoms for future optical experiments.

Acknowledgments

The authors thank the Nano Research Facility of Washington University in St. Louis for providing the dynamic light scattering equipment to measure the lipid droplet diameters. We also thank Professor James Ballard for editing the paper. This work was sponsored in part by National Institutes of Health Grants DP1 EB016986 (NIH Director's Pioneer Award) and R01 CA186567 (NIH Director's Transformative Research Award) as well as National Academies Keck Futures Initiative Grant IS 13.

References

1. B. W. Pogue and M. S. Patterson, "Review of tissue simulating phantom for optical spectroscopy, imaging and dosimetry," *J. Biomed. Opt.* **11**(4), 041102 (2006).
2. J. Linford et al., "Development of a tissue-equivalent phantom for diaphanography," *Med. Phys.* **13**(6), 869–875 (1986).
3. H. J. van Staveren et al., "Light scattering in Intralipid-10% in the wavelength range of 400–1100 nm," *Appl. Opt.* **30**(31), 4507–4514 (1991).
4. A. J. Durkin, S. Jaikumar, and R. Richards-Kortum, "Optically dilute, absorbing, and turbid phantoms for fluorescence spectroscopy of homogeneous and inhomogeneous samples," *Appl. Spectrosc.* **47**(12), 2114–2121 (1993).
5. M. Mark et al., "Multi-modality tissue-mimicking phantom for thermal therapy," *Phys. Med. Biol.* **49**(13), 2767–2778 (2004).
6. U. Sukowski et al., "Preparation of solid phantoms with defined scattering and absorption properties for optical tomography," *Phys. Med. Biol.* **41**(9), 1823–1844 (1996).
7. M. Firbank, M. Oda, and D. T. Delpy, "An improved design for a stable and reproducible phantom material for use in near-infrared spectroscopy and imaging," *Phys. Med. Biol.* **40**(5), 955–961 (1995).
8. M. L. Vernon et al., "Fabrication and characterization of a solid polyurethane phantom for optical imaging through scattering media," *Appl. Opt.* **38**(19), 4247–4251 (1999).
9. R. Bays et al., "Three-dimensional optical phantom and its application in photodynamic therapy," *Lasers Surg. Med.* **21**(3), 227–234 (1997).
10. V. Tuchin, *Tissue Optics: Light Scattering Methods and Instruments for Medical Diagnosis*, SPIE Press, Bellingham, Washington (2007).
11. L. Wang, *Picosecond Kerr Gated Imaging of Phantoms in Turbid Media*, City University of New York, New York (1995).
12. I. Driver et al., "The optical properties of aqueous suspensions of Intralipid, a fat emulsion," *Phys. Med. Biol.* **34**(12), 1927–1930 (1989).
13. P. Di Ninni, F. Martelli, and G. Zaccanti, "Effect of dependent scattering on the optical properties of Intralipid tissue phantoms," *Biomed. Opt. Express* **2**(8), 2265–2278 (2011).
14. P. D. Ninni et al., "Fat emulsions as diffusive reference standards for tissue simulating phantoms?," *Appl. Opt.* **51**(30), 7176–7182 (2012).
15. P. D. Ninni, F. Martelli, and G. Zaccanti, "Intralipid: towards a diffusive reference standard for optical tissue phantoms," *Phys. Med. Biol.* **56**(2), N21–N28 (2011).
16. H. Ding et al., "Determination of refractive indices of porcine skin tissues and Intralipid at eight wavelengths between 325 and 1557 nm," *J. Opt. Soc. Am. A* **22**(6), 1151–1157 (2005).
17. J. Allardice et al., "Standardization of intralipid for light scattering in clinical photodynamic therapy," *Lasers Med. Sci.* **7**(1), 461–465 (1992).
18. X. Xu, H. Liu, and L. V. Wang, "Time-reversed ultrasonically encoded optical focusing into scattering media," *Nat. Photonics* **5**(3), 154–157 (2011).
19. P. Lai et al., "Reflection-mode time-reversed ultrasonically encoded (TRUE) optical focusing into turbid media," *J. Biomed. Opt.* **16**(8), 080505 (2011).
20. A. M. De Grand et al., "Tissue-like phantoms for near-infrared fluorescence imaging system assessment and the training of surgeons," *J. Biomed. Opt.* **11**(1), 014007 (2006).
21. P. Lai, X. Xu, and L. V. Wang, "Ultrasound-modulated optical tomography at new depth," *J. Biomed. Opt.* **17**(6), 066006 (2012).
22. P. Lai et al., "Focused fluorescence excitation with time-reversed ultrasonically encoded light and imaging in thick scattering media," *Laser Phys. Lett.* **10**(7), 075604 (2013).
23. Y. Suzuki et al., "High-sensitivity ultrasound-modulated optical tomography with a photorefractive polymer," *Opt. Lett.* **38**(6), 899–901 (2013).
24. J. R. Cook, R. R. Bouchard, and S. Y. Emelianov, "Tissue-mimicking phantoms for photoacoustic and ultrasonic imaging," *Biomed. Opt. Express* **2**(11), 3193–3206 (2011).
25. R. Michels, F. Foschum, and A. Kienle, "Optical properties of fat emulsions," *Opt. Express* **16**(8), 5907–5925 (2008).
26. S. T. Flock et al., "Optical properties of intralipid: a phantom medium for light propagation studies," *Lasers Surg. Med.* **12**(5), 510–519 (1992).
27. C. Kim et al., "Optical phantoms for ultrasound-modulated optical tomography," *Proc. SPIE* **6870**, 68700M (2008).
28. G. Wagnieres et al., "Design and characterization of a phantom that simultaneously simulates tissue optical properties between 400 and 650 nm," *Proc. SPIE* **2926**, 94–103 (1996).
29. L. Wang and S. L. Jacques, "Use of a laser beam with an oblique angle of incidence to measure the reduced scattering coefficient of a turbid medium," *Appl. Opt.* **34**(13), 2362–2366 (1995).
30. S.-P. Lin et al., "Measurement of tissue optical properties by the use of oblique-incidence optical fiber reflectometry," *Appl. Opt.* **36**(1), 136–143 (1997).
31. B. Cletus et al., "Temperature-dependent optical properties of Intralipid® measured with frequency-domain photon-migration spectroscopy," *J. Biomed. Opt.* **15**(1), 017003 (2010).
32. V. A. McGlone et al., "Measuring optical temperature coefficients of Intralipid®," *Phys. Med. Biol.* **52**(9), 2367–2378 (2007).
33. "Index of refraction of water," in *Handbook of Chemistry and Physics (2000–2001)*, D. R. Lide, Ed., CRC Press, Boca Raton, FL (2000).
34. M. L. Carasso, W. N. Rowlands, and R. A. Kennedy, "Electroacoustic determination of droplet size and zeta potential in concentrated intravenous fat emulsions," *J. Colloid Interface Sci.* **174**(2), 405–413 (1995).
35. E. D. Doktorgrades, *Influence of Lecithin on Structure and Stability of Parenteral Fat Emulsions*, Friedrich-Alexander-Universität Erlangen-Nürnberg, Germany (1998).

Biographies of the authors are not available.